Tumor-targeting nanodelivery enhances the anticancer activity of a novel quinazolinone analogue

Sung Hee Hwang,[1] Antonina Rait,[1] Kathleen F. Pirollo,[1] Qi Zhou,[1] Venkata Mahidhar Yenugonda,[1] Gary M. Chinigo,[2] Milton L. Brown,[2] and Esther H. Chang[1]

[1]Department of Oncology and [2]Departments of Oncology and Neuroscience, Drug Discovery Program, Lombardi Comprehensive Cancer Center, Georgetown University Medical Center, Washington, District of Columbia

Abstract

GMC-5-193 (GMC) is a novel anticancer small-molecule quinazolinone analogue with properties that include antimicrotubule activity and inherent fluorescence. The aim of this study was to produce and optimize a systemically administered liposomal formulation for tumor-targeting delivery of GMC to enhance the anticancer effect of this compound and evaluate its bioefficacy. GMC was encapsulated within a cationic liposome, which was decorated on the surface with an anti-transferrin receptor single-chain antibody fragment (TfRscFv) as the tumor-targeting moiety to form a nanoscale complex (scL/GMC). Confocal imaging of fluorescent GMC uptake in a human melanoma cell line, MDA-MB-435, showed higher cellular uptake of GMC when delivered via the liposome complex compared with free GMC. Delivery of GMC by the tumor-targeting liposome nanoimmunocomplex also resulted in a 3- to 4-fold decrease in IC_{50} values in human cancer cells [DU145 (prostate) and MDA-MB-435] compared with the effects of GMC administered as free GMC. In addition, the GMC nanoimmunocomplex increased the sensitivity of cancer cells to doxorubicin, docetaxel, or mitoxantrone by ~3- to 30-fold. In the MDA435/LCC6 athymic nude mice xenograft lung metastases model, GMC was specifically delivered to tumors by the nanoimmunocomplex. These data show that incorporation of small-molecule therapeutic GMC within the tumor-targeting liposome nanocomplex enhances its anticancer effect. [Mol Cancer Ther 2008;7(3):559–68]

Introduction

Microtubules are self-assembling polymers of α- and β-tubulin heterodimeric proteins and are important cytoskeletal components involved in many cellular events, including maintenance of cellular shape, intracellular transportation, and regulation of motility and mitosis (1, 2). Because of the key role of microtubules in cell mitosis, targeting the microtubule system of eukaryotic cells represents an attractive strategy for the development of anticancer agents. The first Food and Drug Administration–approved antimicrotubule agents were *Vinca* alkaloids, which interact with monomeric tubulin and prevent polymerization (tubulin destabilizer). In contrast, taxanes promote the assembly of microtubules and stabilize microtubule structures (tubulin stabilizer; ref. 3). Both tubulin destabilizers and stabilizers interrupt microtubule dynamics by binding to tubulin, resulting in mitotic arrest that triggers signals for the mitochondrial pathway of apoptosis (4). Although *Vinca* alkaloids (vincristine, vinblastine, and vinorelbine) and taxanes (paclitaxel and docetaxel) are effective anticancer treatments, there are limitations to their use, including toxic side effects and drug resistance through the P-glycoprotein efflux pump (2, 5, 6). In addition, the relatively large molecular weights of these drugs result in complicated synthesis or isolation procedures. Therefore, the search for, and development of, novel small-molecule antimicrotubule agents with improved anticancer effects continues (7, 8).

One approach in the development of improved agents is the modification of the structure of thalidomide. The current small-molecule investigated in this article is a third-generation analogue of thalidomide. Thalidomide was developed in the 1950s as a nontoxic hypnosedative and was widely used to prevent morning sickness in pregnant women until it was withdrawn from the world market because of growing evidence of its teratogenic effects (severe infant limb defects from maternal thalidomide usage; ref. 9). Despite this, thalidomide has shown therapeutic value due to its immunosuppressive and anti-inflammatory effects when used for treating erythema nodosum leprosum, graft-versus-host disease (10–12), HIV-associated cachexia (13), HIV-associated oral aphthous ulcers (9, 14), and a variety of mucocutaneous disorders. In addition, thalidomide has been reported as having anti-angiogenic effects on corneal angiogenesis induced by

Received 8/9/07; revised 11/2/07; accepted 1/11/08.

Grant support: SynerGene Therapeutics research grant (K.F. Pirollo). These studies were conducted in part using the Microscopy and Imaging, Histopathology and Tissue, and Animal Core Facilities supported by National Cancer Institute Cancer Center Support grant and USPHS grants 2P30-CA-51008 and 1 S10 RR 15768-01. This investigation was conducted in part in a facility constructed with support from Research Facilities Improvement grant C06RR14567 from the National Center for Research Resources, NIH.

The costs of publication of this article were defrayed in part by the payment of page charges. This article must therefore be hereby marked *advertisement* in accordance with 18 U.S.C. Section 1734 solely to indicate this fact.

Requests for reprints: Esther H. Chang, Department of Oncology, Lombardi Comprehensive Cancer Center, Georgetown University Medical Center, TRB/E420, 3970 Reservoir Road, North West, Washington, DC 20057-1469. Phone: 202-687-8418; Fax: 202-687-8434. E-mail: change@georgetown.edu

doi:10.1158/1535-7163.MCT-07-0548

vascular endothelial growth factor or basic fibroblast growth factor (15–17). Thalidomide also has been found to be effective in cancers such as relapsed or refractory multiple myeloma (18).

Several groups have been developing thalidomide analogues with more potent antiangiogenic, anti-inflammatory, and anticancer properties (19–25). Our first thalidomide analogue was obtained by replacing the glutaramide ring of thalidomide with phenyl to develop the first active compound showing antiangiogenic and anticancer effects in endothelial cells and prostate cancer cells, respectively (23). Hamel et al. (24) and Hour et al. (25) generated quinazolinones by modifying the phthalimide ring of thalidomide, both resulting in cell death due to inhibition of tubulin function in cells. We optimized the quinazolinone with various substitutions, which led to molecule GMC-5-193 (GMC; Fig. 1).[3] *In vitro* studies using the National Cancer Institute 60-cell line screen, including leukemia, colon cancer, prostate cancer, breast cancer, and renal cancer cell lines, showed the anticancer effects of GMC (1). Moreover, GMC exhibits inherent fluorescence and thereby provides an advantage for detection of the compound by imaging. We hypothesized that the anticancer effects of GMC could be further improved by targeting delivery of the molecule specifically to tumor cells.

Drug delivery systems, such as nanoparticles, microspheres, lipidols, emulsions, activated carbon particles, and liposomes, have been used as carriers of anticancer drugs to alter their pharmacokinetics and thereby reduce toxic side effects and increase antitumor potency (26, 27). Over the past three decades, significant advances have been made in injectable liposomal delivery of anticancer agents and some of them have been introduced into the pharmaceutical market, taking advantage of their biological compatibility. In particular, tumor-targeted immunoliposomes, with the ability to target their payload to tumor cells, are recognized as having an enormous advantage for cancer therapy (28, 29). We have developed a tumor-targeting liposomal delivery system that incorporates an anti-transferrin receptor single-chain antibody fragment (TfRscFv) as the targeting molecule for delivery of gene medicine and small interfering RNA (30–34). Transferrin receptor levels are known to be elevated in various types of cancer cells, including breast, prostate, and pancreatic, and their levels are also correlated with cell proliferation (35, 36). Taking advantage of this, the TfRscFv-liposome complex (scL) has shown preferential targeting of tumor cells. Enhanced expression of scL-delivered genes has been shown in primary tumors as well as metastatic tumors but not in normal tissues (31).

In this study, we employed the tumor-targeting liposomal complex (scL) for delivery of GMC to improve the anticancer effects of this small molecule. Two different human tumor cell lines were used to show the applicability of this approach to diverse types of cancer. Our data reveal that delivery of GMC by means of the tumor-targeting liposomal complex resulted in enhanced cellular uptake of GMC in these tumor cell lines *in vitro* and *in vivo* and increased the cellular response to standard chemotherapeutic agents when compared with free (noncomplexed) GMC.

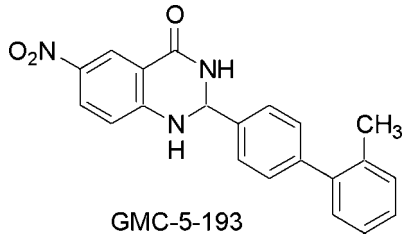

Figure 1. Chemical structure of GMC.

Materials and Methods

Chemicals

The compound GMC was synthesized and its structure (Fig. 1) was confirmed.[3] GMC has a molecular mass of 359.4 Da. A stock solution (2.5 mg/mL) of the compound was prepared in DMSO. 1,2-Dioleoyl-3-trimethylammonium propane and dioleolylphosphatidyl ethanolamine were purchased from Avanti Polar Lipids. Sodium 3′-[1-(phenylamino-carbonyl)-3, 4-tetrazolium]-bis(4-methoxy-6-nitro)benzene sulfonate (XTT) was purchased from Polysciences. *N*-methyl dibenzopyrazine methylsulfate was purchased from Sigma-Aldrich.

Cell Lines and Culture

The human prostate cancer cell line DU145 (ATCC HTB-81) and normal human lung fibroblasts IMR-90 (ATCC CCL-186) were obtained from the American Type Culture Collection. The human melanoma cell line MDA-MB-435 was provided by the Tissue Culture Core Facility at Lombardi Comprehensive Cancer Center, Georgetown University Medical Center. Cells were maintained at 37°C in a 5% CO_2 atmosphere in Eagle's MEM with Earl's salts (DU145 cells) or improved MEM (MDA-MB-435 cells) supplemented with 10% heat-inactivated fetal bovine serum, 2 mmol/L L-glutamine, and 50 μg/mL each of antibiotics, that is, penicillin, streptomycin, and neomycin. IMR-90 was cultured in Eagle's MEM supplemented with 10% heat-inactivated fetal bovine serum, 2 mmol/L L-glutamine, 0.1 mmol/L nonessential amino acids, 1 mmol/L sodium pyruvate, and 50 μg/mL each of the antibiotics. MDA435/LCC6 cells (a gift from Dr. Robert Clarke, Lombardi Comprehensive Cancer Center, Georgetown University Medical Center) were cultured in improved MEM supplemented with 5% heat-inactivated fetal bovine serum, 2 mmol/L L-glutamine, and 50 μg/mL each of penicillin, streptomycin, and neomycin. Eagle's MEM was purchased from MediaTech, and other cell culture media and ingredients were obtained from Biofluids.

[3] Personal communication with Dr. Milton L. Brown, Georgetown University.

Preparation of TfRscFv/LipA/GMC Complex

Cationic liposomal formulation LipA (1,2-dioleoyl-3-trimethylammonium propane/dioleolylphosphatidyl ethanolamine at a 1:1 molar ratio) was prepared using the ethanol injection method as described previously (31). TfRscFv/LipA/GMC (scL/GMC) complex was prepared as described previously (32). The molar ratio of LipA to GMC was 1:1. For *in vitro* experiments, the complex was further diluted with serum-free medium. For animal injections, 50% dextrose was added to each sample to a final concentration of 5% dextrose. The size of the complex was determined by dynamic light scattering at 25°C with a Zetasizer Nano ZS System. The mean particle size of scL/GMC in water was 168.9 ± 6.1 nm.

In vitro Confocal Imaging

For confocal imaging, 5.0×10^4 MDA-MB-435 cells per well were seeded on glass coverslips in a 24-well plate. Twenty-four hours later, cells were washed with serum-free medium, treated with scL/GMC complex or free GMC, and incubated for 6 h. After treatment, cells were washed twice with PBS, fixed with 4% paraformaldehyde in PBS for 15 min at room temperature, and washed again with PBS. For nuclear staining, blue fluorescent counterstain reagent 4′,6-diamidino-2-phenylindole (DAPI) in Select FX Nuclear Labeling Kit for fixed cells (Molecular Probes) was used according to the manufacturer's protocol. Cells on glass coverslips were then mounted on glass slides using Antifade mounting solution (ProLong Antifade Kit, Molecular Probes). For imaging, an Olympus FLUOVIEW-300 laser scanning confocal system with ×60 oil immersion objective was used. For the 4′,6-diamidino-2-phenylindole, a 405 nm blue diode laser was used to excite the sample. The emitted light from the sample was directed with a mirror through a 430 to 460 nm band-pass filter and captured by the PMT detector. For the GMC, the 488 nm blue line of an argon laser was used to excite the sample. The emitted light from the sample was directed with a mirror through a 505 to 525 nm band-pass filter and captured by the PMT detector.

In vitro Cell Viability

For *in vitro* cell survival studies, 5.5×10^3 DU145 or MDA-MB-435 cells per well in 100 μL of the appropriate growth medium were plated in a 96-well plate. After 24 h, the medium was replaced with serum-free medium, overlaid with 100 μL of increasing concentrations of either scL/GMC complex, unliganded complex (L/GMC), free GMC, or LipA only in serum-free medium, incubated for 5 h, and then supplemented with fetal bovine serum. After incubation for an additional 43 h at 37°C in a humidified atmosphere containing 5% CO_2, the wells were washed with improved MEM without phenol red and a cell viability XTT-based assay was done as described previously (37). Formazan absorbance, which correlates to cell viability, was measured at 450 nm using a microplate reader (Ultramark, Microplate Imaging System, Bio-Rad). The IC_{50} value (the concentration yielding 50% growth inhibition) was interpolated from the graph of the log of drug concentration versus the fraction of surviving cells.

In vitro Chemosensitization

For the chemosensitization study, 4.5×10^3 DU145, MDA-MB-435, or IMR-90 cells per well in 100 μL medium were seeded in a 96-well plate. After 24 h, the medium was replaced with serum-free medium and overlaid with 100 μL of either scL/GMC complex or free GMC, in each case the concentration of GMC being either 1 or 1.25 μmol/L. Cells were then incubated at 37°C for 5 h, after which fetal bovine serum was added to each well and incubated an additional 19 h. The appropriate supplemented medium was then added either with or without chemotherapeutics in increasing concentrations and incubation continued for ~48 h. Chemotherapeutic drugs used were doxorubicin (Bedford Laboratories), docetaxel (Taxotere; Aventis Pharmaceuticals), and mitoxantrone (Osi Pharmaceuticals). XTT assays were done to assess the degree of sensitization to the chemotherapeutics, and IC_{50} values were calculated. Fold sensitization was determined as follows: IC_{50} chemotherapeutic agent only / IC_{50} each combination treatment.

In vivo Tumor Targeting

For *in vivo* studies, human melanoma MDA435/LCC6 cells (derived from MDA-MB-435 cells) were used to generate lung metastatic tumors. MDA435/LCC6 cells (8×10^6 cells per mouse) suspended in PBS were injected i.v. into the tail vein of 5-week-old female athymic nude mice. Ten to 12 weeks after injection, MDA435/LCC6 xenograft lung metastases were established. The mice were injected i.v. with 9 mg/kg GMC as either free GMC or scL/GMC. Three hours after injection, the liver and lung were excised and examined under a fluorescence microscope (Nikon SMZ-1500 EPI-Fluorescence stereoscope system). Images were acquired with an Hg lamp source using a ''FITC-like'' set of filters [excitation (nm), 480/40; dichroic (nm), 505 nm; emission (nm), BA535/50]. The care and use of laboratory animals have been approved by the Georgetown University Animal Care and Use Committee.

Results

In vitro Confocal Imaging

Taking advantage of the inherent fluorescence of GMC, confocal imaging was used to compare the internalization of GMC when delivered as free GMC with that when complexed with the targeted liposome (scL/GMC). MDA-MB-435 cells were treated for 6 h with either free GMC or scL/GMC, washed with PBS, fixed with 4% paraformaldehyde in PBS, and visualized by confocal microscopy. At 6 h post-transfection, green fluorescence was greater in cells treated with scL/GMC than in cells treated with free GMC (Fig. 2), representing ~3-fold increase in intensity (arbitrary values measured by Metamorph: 220 for scL/GMC and 72 for free GMC). Differential interference contrast (DIC) images revealed the morphology of the cells. GMC green fluorescence was distributed throughout cells treated with either free GMC or scL/GMC, including in the cytoplasm and the nucleus. These results indicate that GMC is more easily taken up by MDA-MB-435 cells when delivered by means of the targeted liposomal complex.

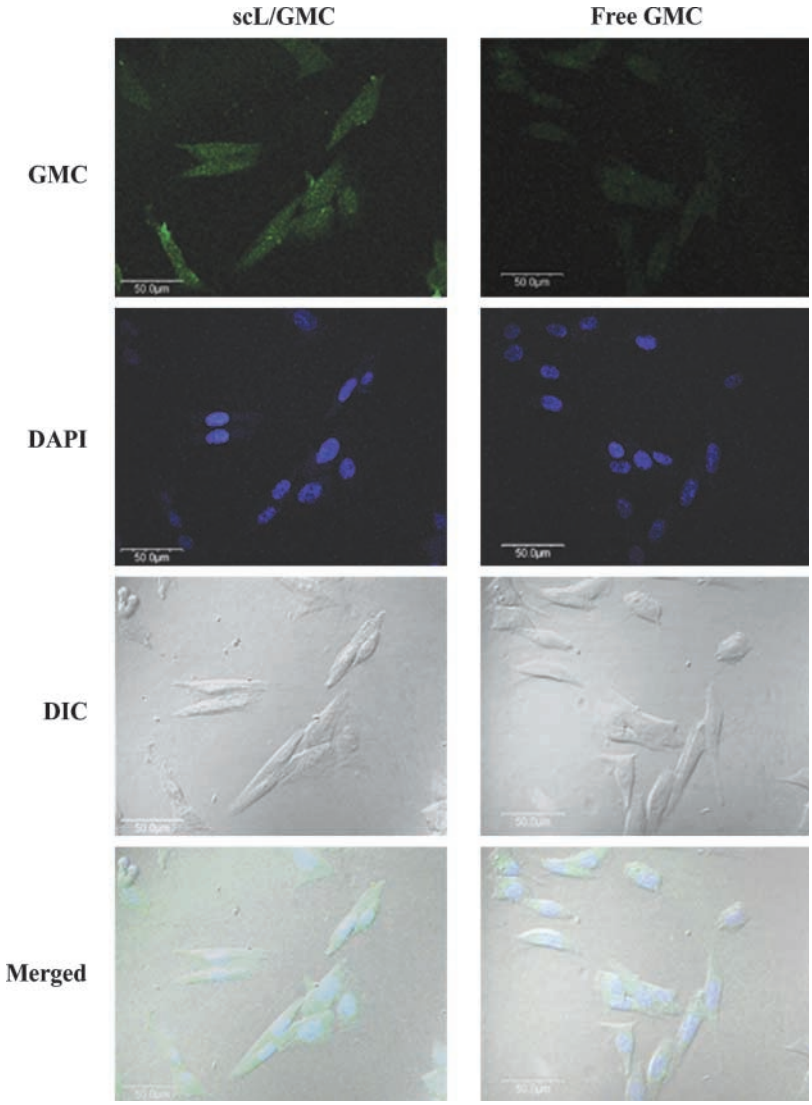

Figure 2. *In vitro* comparison of uptake in human melanoma cells of free GMC and scL/GMC complex. MDA-MB-435 cells (5×10^4) per well were seeded on glass slides in a 24-well plate and after 24 h were treated with scL/GMC complex or free GMC for 6 h. After treatment, cells were washed with PBS, fixed with 4% paraformaldehyde in PBS, stained with DAPI, and mounted on the glass slides. The Olympus FLUOVIEW-300 laser scanning confocal system was used to visualize fluorescence. Magnification, ×60.

In vitro Cytotoxicity of scL/GMC Complex

Molar ratios of GMC to targeted liposome (scL) were determined for optimal efficient delivery to cells. The dose response of scL/GMC on MDA-MB-435 cells was determined. As shown in Fig. 3A, IC_{50} values of GMC-treated MDA-MB-435 cells were 12 μmol/L for free GMC and 3 μmol/L for scL/GMC, indicating a 4-fold increase in cell killing after treatment with the targeted liposome-delivered GMC (scL/GMC). Treatment of cells with liposome alone (LipA), in concentrations up to 6 μmol/L, did not result in any cytotoxicity. Only at the highest concentration of LipA (LipA concentration equivalent to 50 μmol/L scL/GMC) was some growth inhibition observed, that is, 50% growth inhibition. Similar results were obtained with DU145 cells (Fig. 3B), showing a 3-fold increase in cell death after treatment with scL/GMC compared with free GMC (IC_{50}, 4 and 12 μmol/L, respectively; Fig. 3B). Moreover, the importance of the tumor-targeting ligand is shown in Fig. 3C with MDA-MB-435 cells. Whereas there was very little difference observed between the free GMC (IC_{50}, 12 μmol/L) and the unliganded complex (L/GMC; IC_{50}, 9 μmol/L), there is a significant difference in IC_{50} values between the complex with and the complex without the TfRscFv targeting moiety. The IC_{50} value with the unliganded complex (L/GMC) is 9 μmol/L, whereas that of the full complex is 1.9 μmol/L, a >4-fold increase in cell killing when the ligand is included in the complex.

In vitro Chemosensitization by the scL/GMC Nanoimmunocomplex

We have shown previously that GMC disrupts and destabilizes microtubules.[3] In view of this, we hypothesized that the combination of GMC with conventional chemotherapeutics would enhance the anticancer effects of conventional chemotherapies. First, the ability of scL/GMC to sensitize MDA-MB-435 cells to docetaxel was explored (Fig. 4A). Docetaxel is a microtubule-targeted, tubulin-polymerizing agent that has shown a high level of clinical activity. Cells treated with a combination of liposome

(LipA) and docetaxel showed an IC_{50} value (9 nmol/L) similar to that of cells treated with docetaxel only, revealing a lack of toxicity of the liposomes themselves. Whereas treatment with 1.25 μmol/L free GMC resulted in an ~21-fold increase in sensitization of MDA-MB-435 cells to docetaxel-induced cell death (IC_{50}, 0.43 nmol/L), encapsulation of the same concentration of GMC (1.25 μmol/L) within the targeted liposome nanocomplex resulted in an 80% reduction in cell survival even without treatment with docetaxel; therefore, the IC_{50} was unable to be determined. In view of this, another experiment was done using a lower concentration of GMC (1 μmol/L; Fig. 4B). As in the previous experiment, administration of docetaxel alone and LipA plus docetaxel resulted in similar IC_{50} values (12 and 9 nmol/L, respectively). GMC (1 μmol/L) delivered by the targeted liposome (scL/GMC) resulted in a dramatic sensitization of MDA-MB-435 cells to docetaxel (Fig. 4B), exhibiting an IC_{50} value of 0.4 nmol/L. This represents a 30-fold increase in sensitization when compared with cells treated with docetaxel only and a 3-fold increase in sensitization over cells treated with free GMC and docetaxel (IC_{50}, 1.2 nmol/L).

GMC-induced sensitization of cancer cells to the chemotherapeutic agents doxorubicin and mitoxantrone was also evaluated. Doxorubicin is used to treat a variety of cancers including breast, ovarian, lung, thyroid, gastric, transitional

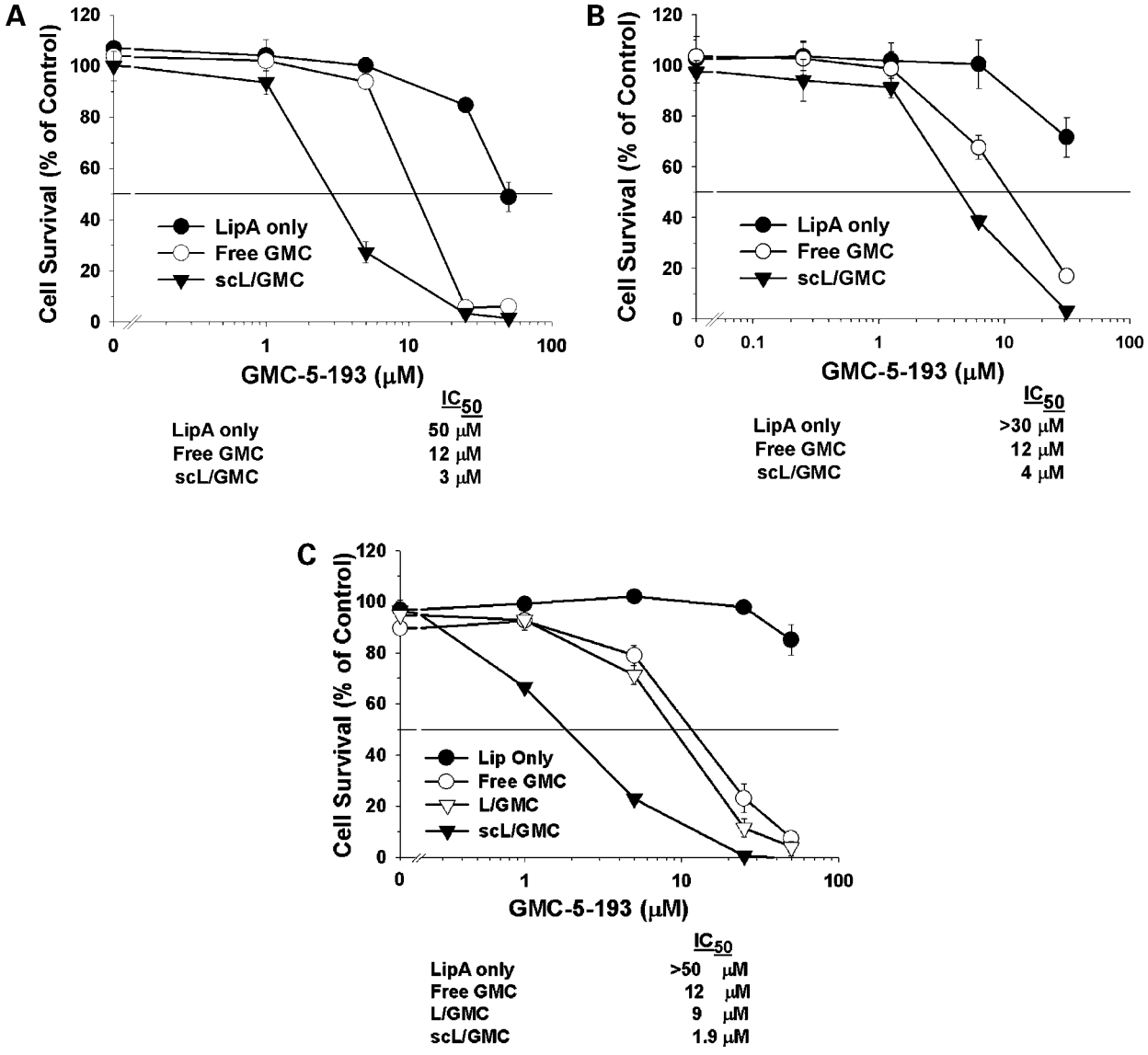

Figure 3. Effect of GMC nanoimmunocomplex (scL/GMC) on MDA-MB-435 and DU145 cells. MDA-MB-435 cells (**A** and **C**) or DU145 cells (**B**) were plated at 5.5×10^3 per well in a 96-well plate and treated after 24 h with scL/GMC, free GMC, unliganded complex (L/GMC), or LipA alone. XTT assays were done 48 h after treatment to assess cytotoxicity. Points, mean of triplicate samples; bars, SD. The IC_{50} value (the concentration yielding 50% growth inhibition) was interpolated from the graph of the log of drug concentration versus the fraction of surviving cells.

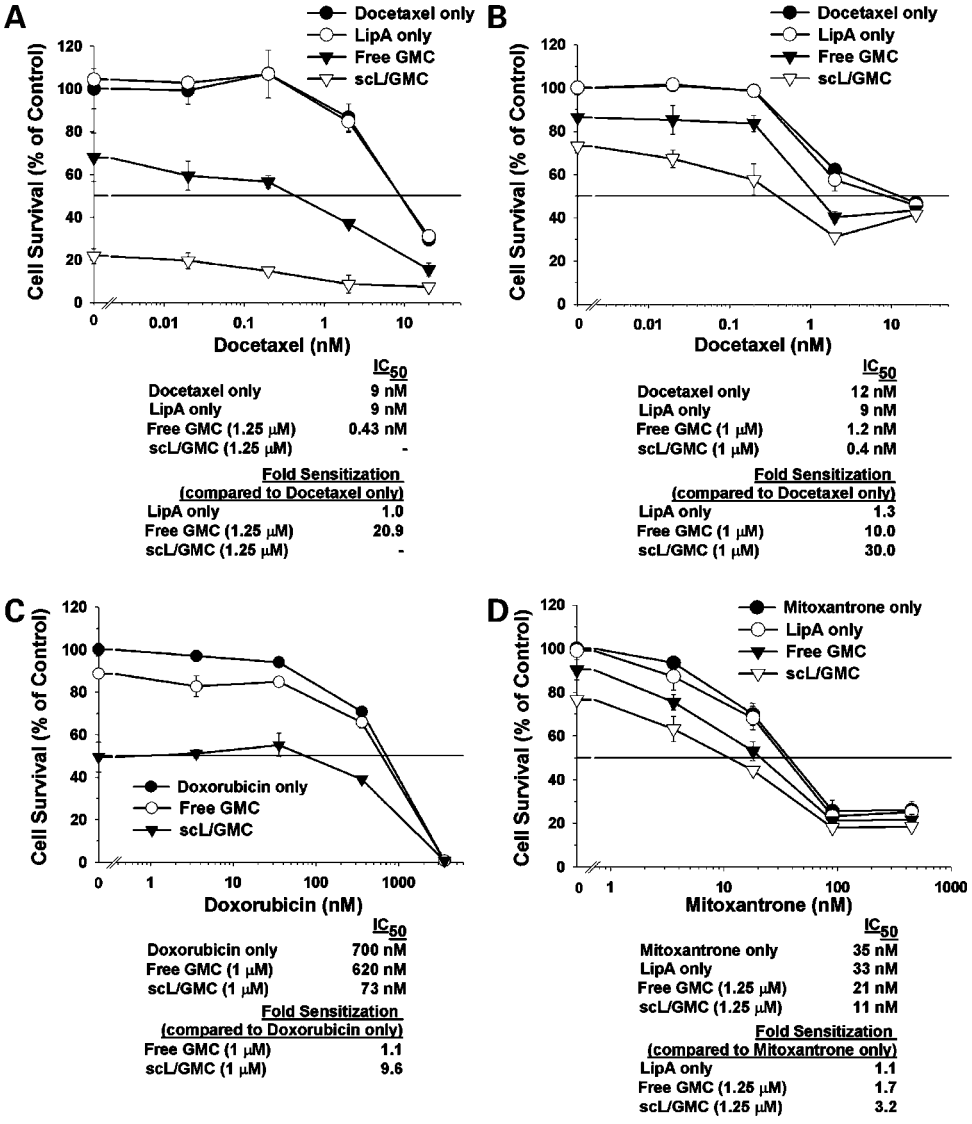

Figure 4. Effect of GMC nanoimmunocomplex (scL/GMC) on sensitization of human melanoma or prostate cancer cells to docetaxel, doxorubicin, or mitoxantrone. MDA-MB-435 cells (**A**-**C**) or DU145 cells (**D**) were plated at 4.5×10^3 per well in a 96-well plate and after 24 h treated with scL/GMC complex. The concentration of GMC was 1 μmol/L (**B** and **C**) or 1.25 μmol/L (**A** and **D**). After 24 h, docetaxel (**A** and **B**), doxorubicin (**C**), or mitoxantrone (**D**) was added in increasing concentrations. After 48 h, XTT assays were done to assess cell viability in response to treatments. Points, mean of triplicate samples; bars, SD. The IC_{50} value (the concentration yielding 50% growth inhibition) was interpolated from the graph of the log of drug concentration versus the fraction of surviving cells. Fold sensitization = IC_{50} chemotherapeutic agent only / IC_{50} each combination treatment.

cell bladder cancer, soft tissue and osteogenic sarcomas, neuroblastoma, Wilms' tumor, Hodgkin's and non-Hodgkin's lymphoma, acute myeloblastic leukemia, acute lymphoblastic leukemia, and even Kaposi's sarcoma related to AIDS. *In vitro* studies show doxorubicin to be potent in inducing cell death in various cancer cell lines including MDA-MB-435. Mitoxantrone, a synthetic antineoplastic anthracenedione, was also used in these studies due to its use in combination with corticosteroids as a first-step chemotherapy for the treatment of patients with advanced hormone-refractory prostate cancer. As shown in Fig. 4C, MDA-MB-435 cells treated with doxorubicin only exhibited an IC_{50} of 700 nmol/L, whereas GMC (1 μmol/L), either in free form (free GMC) or complexed with the targeted liposome (scL/GMC), sensitized cells to doxorubicin-induced death, with IC_{50} values of 620 and 73 nmol/L, respectively. Thus, GMC delivered by the targeted liposome resulted in a 9.6-fold increased sensitization to doxorubicin, whereas free GMC resulted in a 1.1-fold increase in sensitization to doxorubicin (Fig. 4C). Figure 4D shows that DU145 cells treated with either free GMC or scL/GMC (1.25 μmol/L GMC) were also sensitized to mitoxantrone-induced cell death, exhibiting IC_{50} values of 21 and 11 nmol/L, respectively, and representing a greater increase in sensitization by scL/GMC (3.2-fold) than by free GMC (1.7-fold) when compared with mitoxantrone treatment only (IC_{50}, 35 nmol/L; Fig. 4D).

To confirm that the increases in sensitization of cells to chemotherapeutic drugs were not due to nonspecific cytotoxicity from GMC or scL/GMC, the normal human lung fibroblast cell line, IMR-90, was used (Fig. 5A and B). IMR-90 cells, when treated with docetaxel or mitoxantrone, showed no appreciable sensitization by LipA, free GMC, or scL/GMC when compared with the cells treated with docetaxel or mitoxantrone only.

These *in vitro* data support the observation that GMC delivered to cells by the targeted liposome sensitizes cancer cells to conventional chemotherapeutics more effectively than when delivered as free GMC.

In vivo Tumor Targeting

We have shown previously that our TfRscFv-liposome can deliver DNA preferentially to tumor cells after systemic administration (31). The following studies were done to determine whether the TfRscFv-liposome could deliver a different class of payload, that is, a small molecule, also preferentially to tumor cells after systemic administration. Athymic nude mice carrying MDA435/LCC6 xenograft metastatic tumors, primarily in the lung, were injected i.v. with free GMC or scL/GMC at a concentration of GMC of 9 mg/kg/mouse. Three hours after injection, liver and lung were excised and examined under a fluorescence microscope. Figure 6 shows the same field photographed in bright-field (*left*) or with fluorescence (*right*). In the bright-field image of the mouse treated with free GMC, large tumors can be observed throughout the lung, but the fluorescent image shows only weak fluorescence in all the tissues. In the bright-field image of the mouse injected with scL/GMC complex, metastases are distinguishable as being denser than the lighter bubbly appearance of the normal lung tissue, and the fluorescent image shows the clearly discernible fluorescence of GMC in these lung metastases. Thus, GMC fluorescence in the lung metastases is ~2-fold stronger in this mouse than in the mouse treated with free GMC when measured by Metamorph, representing a greater amount of GMC present in these metastases. In contrast to these images, the normal liver shows only weak fluorescence. These results show that tumor-specific uptake of GMC after systemic administration is enhanced when GMC is delivered by the targeted liposome complex.

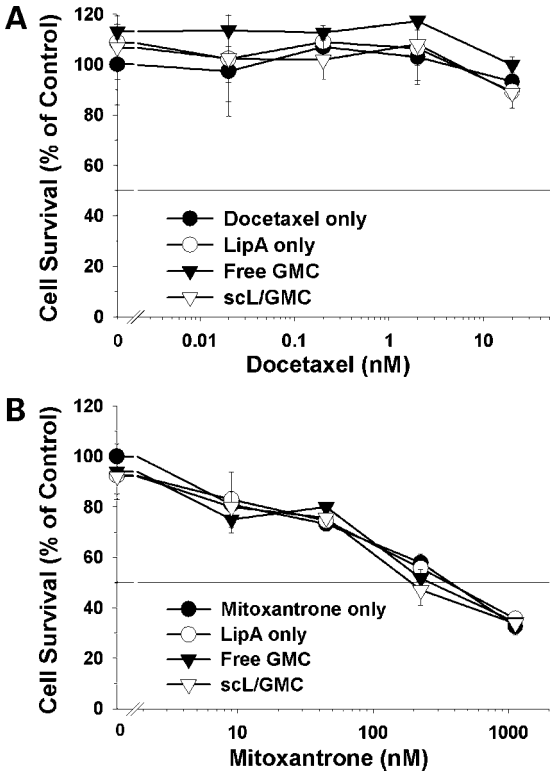

Figure 5. Effect of GMC nanoimmunocomplex (scL/GMC) on sensitization of IMR-90 to docetaxel or mitoxantrone. Normal human fibroblast cells (IMR-90) were plated at 4.5×10^3 per well in a 96-well plate and after 24 h treated with scL/GMC complex. The concentration of GMC was 1.25 μmol/L. After 24 h, docetaxel (**A**) or mitoxantrone (**B**) was added in increasing concentrations. After 48 h, XTT assays were done to assess cell viability in response to treatments. Points, mean of triplicate samples; bars, SD. The IC_{50} value (the concentration yielding 50% growth inhibition) was interpolated from the graph of the log of drug concentration versus the fraction of surviving cells. Fold sensitization = IC_{50} chemotherapeutic agent only / IC_{50} each combination treatment.

Discussion

Several studies using thalidomide analogues suggest that their antiproliferative effect in several types of cancer cells may be due to inhibition of tubulin polymerization (25, 26). These analogues initiate formation of abnormal mitotic spindles in cancer cells. Our previous study clearly showed that GMC, a thalidomide analogue, inhibits human cancer cell proliferation.[3] The potency of this molecule is similar to other well-known antimitotic agents such as colchicine, combretastatin, and *Vinca* alkaloids. These compounds are tubulin destabilizers and have been found to inhibit the function of the mitotic spindle. Most, however, have been toxic with limited ability to track their intracellular mechanism. GMC is a fluorescent tubulin destabilizer that is advantageous for intracellular and intratumoral detection.

In vitro, in both human melanoma (MDA-MB-435) and prostate (DU145) cell lines, dose-response studies revealed IC_{50} values of free GMC of 12 μmol/L after treatment for 2 days. Delivery of GMC by the tumor-targeting liposome nanodelivery system (scL/GMC) reduced the IC_{50} values in MDA-MB-435 and DU145 cells by 4- and 3-fold, respectively (Fig. 3), revealing an increase in sensitivity of cells to GMC. At these IC_{50} values, the liposome itself did not show any toxic effects on both cell lines. Figure 3C shows that the increase in the effectiveness of GMC in inducing cell death results from enhanced cellular uptake of GMC when delivered by the targeted liposome. Transferrin receptors are elevated in DU145 and MDA-MB-435 cells (35, 36) and have been shown to play a key role in receptor-mediated endocytosis of TfRscFv-liposomes (30–34), also resulting in increased cellular uptake. Thus, in this study, confocal images of MDA-MB-435 cells treated with the small molecule revealed that GMC can be more efficiently taken up by the cells when delivered by the targeted liposome than when delivered as free GMC (Fig. 2), as shown by the ~3-fold increase in green fluorescence in cells treated with scL/GMC than in cells treated with free GMC. These data are similar to our previous reports showing that incorporation of the tumor-targeting moiety, TfRscFv, in the complex enhanced tumor-specific cellular uptake, systemic delivery of payload to both primary tumor and metastases, and efficacy (30–34).

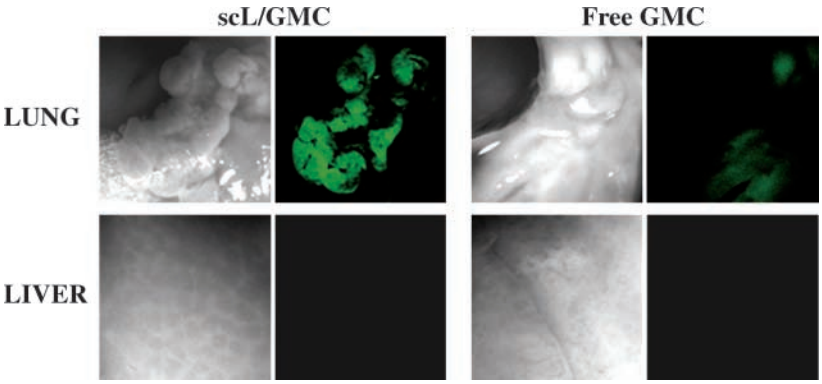

Figure 6. Comparison of tumor-specific uptake of systemically administered free or scL encapsulated GMC. Athymic nude mice carrying MDA435/LCC6 lung xenograft tumors were injected i.v. with free GMC or scL/GMC at 9 mg/kg GMC/mouse. Three hours after injection, the liver and the lung were excised and examined under a microscope. The Nikon SMZ-1500 EPI-Fluorescence stereoscope system was used to image tissue fluorescence.

Combination therapy, in which cancer patients are routinely treated with a combination of cancer therapies, has been shown as having many advantages over single-agent therapies. A combination of antimicrotubule agents docetaxel and estramustine has been evaluated in the treatment of metastatic, androgen-independent prostate cancer with positive results (38). Combination therapy comprising antimicrotubule agents plus doxorubicin or cisplatin is proposed as an effective regimen for breast cancers (39, 40). In addition, thalidomide, the parent compound of GMC, is being used more extensively in the treatment of various cancers such as multiple myeloma (41), colon cancer (42), and prostate cancer (43) in combination with cyclophosphamide, dexamethasone, capecitabine, irinotecan, or docetaxel. Combining dacarbazine and thalidomide has been reported as a promising strategy for the treatment of melanoma (44). Similarly, our current studies have shown increased sensitization of cells to conventional chemotherapeutics by combining treatment with the thalidomide analogue GMC.

GMC was shown to increase sensitization of MDA-MB-435 and DU145 cells to docetaxel/doxorubicin and mitoxantrone, respectively. However, MDA-MB-435 cells exhibited greater sensitivity to docetaxel than to doxorubicin (IC_{50}, 9-12 and 700 nmol/L, respectively), and a similar greater sensitivity to combination treatment with both GMC and docetaxel, than with both GMC and doxorubicin. It is not clear why the two chemotherapeutic drugs exhibited such differences in inducing cell death in the MDA-MB-435 cells, although this could be a cell-specific phenomenon. It is interesting to note that synergistic combinations of taxanes and antimicrotubule agents have been explored in several studies. Although expression of the *mdr1* gene has been known shown to be the main cause of drug resistance, several studies have shown that cancer cells resistant to microtubule-targeting agents include alteration in microtubule structure due to changes in β-tubulin isotype content and tubulin content (2). An increase in β-tubulin III content has been repeatedly related to taxane resistance *in vitro* (2, 45) and in clinical settings. Recent clinical evidence supports β-tubulin III content as a marker of poor response to taxanes in different cancers, including non-small cell lung cancer (46), breast cancer (47), and ovarian cancer (48). Moreover, when paclitaxel-resistant lung cancer cells, A549-T24, were treated with antisense oligonucleotides to β-tubulin III, a 39% increase in sensitivity to paclitaxel was shown (49). Similarly, a synergistic effect between the tubulin stabilizer paclitaxel and the tubulin destabilizer vinorelbine against human melanoma lines was reported (50). Unfortunately, a combination of these chemotherapeutics is not currently in clinical use due to severe neurotoxic effects (51). In view of the above, the distinguishable synergistic effect of the scL/GMC complex in combination with docetaxel in MDA-MB-435 cells may be due to the fact that GMC targets β-tubulin III, thereby increasing sensitivity to docetaxel.

In our experiments, the effect of GMC on tumor cells was dramatically different from the effect of GMC on normal human lung fibroblasts IMR-90 under the same conditions, in that the normal lung fibroblasts showed no significant sensitization to chemotherapeutics when treated with either free GMC or scL/GMC. These data indicate that TfRscFv-targeted liposomal delivery targets the GMC complex to cancer cells but not to normal cells, thereby increasing its therapeutic index. The current *in vitro* experiments show that although GMC sensitizes cancer cells to conventional chemotherapeutic drugs the effect of GMC is greatly enhanced when delivered by the targeted liposome. Therefore, GMC nanoimmunocomplexes (scL/GMC) in combination with conventional chemotherapeutics may likely result in distinct advantages over treatment with free GMC or with conventional chemotherapeutics only and may permit a reduction in the effective dose of chemotherapeutic with a subsequent reduction in the incidence of adverse side effects.

The primary focus of this study was to deliver GMC specifically to tumor cells *in vivo* after systemic administration. scL/GMC administered i.v. to athymic nude mice carrying MDA435/LCC6 xenograft metastatic tumors primarily in the lung resulted in GMC delivery specifically to the metastatic tumor cells, to a greater extent than free GMC administered i.v., as determined by observation of intensity of green fluorescence in the lung metastases. Tumor-specific uptake of GMC after systemic administration of scL/GMC was clearly observed, correlating with our previous reports showing tumor-targeting delivery of gene medicine (30–34).

When it is established that scL/GMC could be delivered to metastatic tumors *in vivo*, the next step will be to determine antitumor efficacy. As discussed previously, GMC exhibits antimicrotubule activity, and it is also possible that the effectiveness of the small molecule as a cancer treatment may be due to antiangiogenic activity. Thalidomide is known to have antiangiogenic activity (16) and several thalidomide analogues have also been reported as exhibiting antiangiogenic activity (19, 23). As a thalidomide analogue, it is possible that GMC may also exhibit antiangiogenic activity, which may work cooperatively with antimicrotubule activity for cancer treatment, although further study on its mechanism of action is required.

These studies have shown efficient and tumor-specific targeted delivery of the novel anticancer small-molecule GMC. GMC can be delivered to tumors specifically and more efficiently when incorporated into a tumor-targeting liposome complex than as a free small molecule. As a result, a significantly higher level of *in vitro* chemosensitization in human melanoma and prostate cancer cells was evident when GMC was delivered by the targeted liposome nanodelivery system than when delivered as free GMC. Similarly, treatment of cancer cells with scL/GMC more efficiently sensitized cells to the chemotherapeutics docetaxel, doxorubicin, or mitoxantrone. In contrast, there was no increase in toxicity in normal lung fibroblasts. These data also showed a synergistic effect between the nano-immunoliposome complexed small molecule and docetaxel in a melanoma lung metastases animal model. In humans, a substantial advantage to such a synergistic combination treatment would be the possibility of reducing the dose of conventional chemotherapeutic agents while maintaining or even increasing their effectiveness, with a concomitant decrease in toxic side effects, thereby increasing the quality of life for cancer patients.

Acknowledgments

We thank Dr. Leanne Sleer for advice and assistance in preparation of this article and Guillermo Palchik and Dr. Thane Govindan for assistance with confocal and fluorescence microscopy.

References

1. Margolis RL, Wilson L. Microtubule treadmilling: what goes around comes around. BioEssays 1998;20:830 – 6.

2. Dumontet C, Sikic B. Mechanisms of action of and resistance to antimicrotubulin agents: microtubule dynamics, drug transport and cell death. J Clin Oncol 1999;7:1061 – 70.

3. Rowinsky EK, Donehower RC. The clinical pharmacology and use of antimicrotubule agents in cancer chemotherapeutics. Pharmacol Ther 1991;52:35 – 84.

4. Bhalla KN. Microtubule-targeted anticancer agents and apoptosis. Oncogene 2003;22:9075 – 86.

5. Huang Y, Ibarado AM, Reed JC, et al. Co-expression of several molecular mechanisms of multidrug resistance and their significance for paclitaxel cytotoxicity in human AML HL-60 cells. Leukemia 1997;11: 253 – 7.

6. Dey S, Ramachandra M, Pastan I, Gottesman MM, Ambudkar SV. Evidence for two nonidentical drug interaction sites in the human P-glycoprotein. Proc Natl Acad Sci U S A 1997;94:10594 – 9.

7. Ku CC, Hsieh HP, Pan WY, et al. BPR0L075, a novel synthetic indole compound with antimitotic activity in human cancer cells, exerts effective antitumoral activity *in vivo*. Cancer Res 2004;64:4621 – 8.

8. Li JN, Song DQ, Lin YH, et al. Inhibition of microtubule polymerization by 3-bromopropionylamino benzoylurea (JIMB01), a new cancericidal tubulin ligand. Biochem Pharmacol 2003;65:1691 – 9.

9. Tseng S, Pak G, Washenik K, Pomeranz MK, Shupack JL. Rediscovering thalidomide: a review of its mechanism of action, side effects, and potential uses. J Am Acad Dermatol 1996;35:969 – 79.

10. Vogelsang GB, Hess AD, Gordon G, Santos GW. Treatment and prevention of acute graft-versus-host disease with thalidomide in a rat model. Transplantation 1986;41:644 – 7.

11. McCarthy DM, Kanfer EJ, Barrett AJ. Thalidomide for the therapy of graft-versus-host disease following allogeneic bone marrow transplantation. Biomed Pharmacother 1989;43:693 – 7.

12. Forsyth CJ, Cremer PD, Torzillo P, Iland HJ, Young GA. Thalidomide responsive chronic pulmonary GVHD. Bone Marrow Transplant 1996;17: 291 – 3.

13. Reyes-Teran G, Sierra-Madero JG, Martinez DCV, et al. Effects of thalidomide on HIV-associated wasting syndrome: a randomized, double-blind, placebo-controlled clinical trial. AIDS 1996;10:1501 – 7.

14. Jacobson JM, Greenspan JS, Spritzler J, et al. Thalidomide for the treatment of oral aphthous ulcers in patients with human immunodeficiency virus infection. National Institute of Allergy and Infectious Diseases AIDS Clinical Trials Group. N Eng J Med 1997;336:1487 – 93.

15. Kruse FE, Joussen AM, Rohrschneider K, Becker MD, Völcker HE. Thalidomide inhibits corneal angiogenesis induced by vascular endothelial growth factor. Graefes Arch Clin Exp Ophthalmol 1998;236:461 – 6.

16. D'Amato RJ, Loughnan MS, Flynn E, Folkman J. Thalidomide is an inhibitor of angiogenesis. Proc Nat Acad Sci U S A 1994;91:4082 – 5.

17. Kenyon BM, Browne F, D'Amato RJ. Effects of thalidomide and related metabolites in a mouse corneal model of neovascularization. Exp Eye Res 1997;64:971 – 8.

18. Singhal S, Mehta J, Desikan R, et al. Antitumor activity of thalidomide in refractory multiple myeloma. N Eng J Med 1999;341:1565 – 71.

19. Ng SS, Gutschow M, Weiss M, et al. Antiangiogenic activity of *N*-substituted and tetrafluorinated thalidomide analogues. Cancer Res 2003;63:3189 – 94.

20. Dredge K, Marriott JB, Macdonald CD, et al. Novel thalidomide analogues display anti-angiogenic activity independently of immunomodulatory effects. Br J Cancer 2002;87:1166 – 72.

21. Lima LM, Castro P, Machado AL, et al. Synthesis and anti-inflammatory activity of phthalimide derivatives, designed as new thalidomide analogues. Bioorg Med Chem 2002;10:3067 – 73.

22. Dredge K, Marriott JB, Dalgleish AG. Immunological effects of thalidomide and its chemical and functional analogs. Crit Rev Immunol 2002;22:425 – 37.

23. Capitosti SM, Hansen TP, Brown ML. Thalidomide analogues demonstrate dual inhibition of both angiogenesis and prostate cancer. Bioorg Med Chem 2004;12:327 – 36.

24. Hamel E, Lin CM, Plowman J, Wang HK, Lee KH, Paull KD. Antitumor 2,3-dihydro-2-(aryl)-4(1H)-quinazolinone derivatives. Interactions with tubulin. Biochem Pharmacol 1996;51:53 – 9.

25. Hour MJ, Huang LJ, Kuo SC, et al. 6-Alkylamino- and 2,3-dihydro-3′-methoxy-2-phenyl-4-quinazolinones and related compounds: their synthesis, cytotoxicity, and inhibition of tubulin polymerization. J Med Chem 2000;43:4479 – 87.

26. Marinina J, Shenderova A, Mallery SR, Schwendeman SP. Stabilization of *Vinca* alkaloids encapsulated in poly(lactide-co-glycolide) microspheres. Pharm Res 2000;17:677 – 83.

27. Sachdeva MS. Drug targeting systems for cancer chemotherapy. Expert Opin Investig Drugs 1998;7:1849 – 64.

28. Sapra P, Moase EH, Ma J, Allen TM. Improved therapeutic responses in a xenograft model of human B lymphoma (Namalwa) for liposomal vincristine versus liposomal doxorubicin targeted via anti-CD19 IgG2a or Fab fragments. Clin Cancer Res 2004;10:1100 – 11.

29. Mastrobattista E, Koning GA, Storm G. Immunoliposomes for the targeted delivery of antitumor drugs. Adv Drug Deliv Rev 1999;40:103 – 27.

30. Xu L, Tang WH, Huang CC, et al. Systemic p53 gene therapy of cancer with immunolipoplexes targeted by anti-transferrin receptor scFv. Mol Med 2001;7:723 – 34.

31. Xu L, Huang CC, Huang W, et al. Systemic tumor-targeted gene delivery by anti-transferrin receptor scFv-immunoliposomes. Mol Cancer Ther 2002;1:337 – 46.

32. Yu W, Pirollo KF, Yu B, et al. Enhanced transfection efficiency of a systemically delivered tumor-targeting immunolipoplex by inclusion of a pH-sensitive histidylated oligolysine peptide. Nucleic Acids Res 2004; 32:e48.

33. Pirollo KF, Zon G, Rait A, et al. Tumor-targeting nanoimmunoliposome complex for short interfering RNA delivery. Hum Gene Ther 2006;17: 117 – 24.

34. Pirollo KF, Rait A, Zhou Q, et al. Materializing the potential of small interfering RNA via a tumor-targeting nanodelivery system. Cancer Res 2007;67:2938 – 43.

35. Keer HN, Kozlowski JM, Tsai MC. Elevated transferrin receptor content in human prostate cancer cell lines assessed *in vitro* and *in vivo*. J Urol 1990;143:381 – 5.

36. Inoue T, Cavanaugh PG, Steck PA, Brunner N, Nicolson GL. Differences in transferrin response and numbers of transferrin receptors in rat and human mammary carcinoma lines of different metastatic potentials. J Cell Physiol 1993;156:212 – 7.

37. Rait A, Pirollo KF, Rait V, et al. Inhibitory effects of the combination of HER-2 antisense oligonucleotide and chemotherapeutic agents used for the treatment of human breast cancer. Cancer Gene Ther 2001;8: 728 – 39.

38. Petrylak DP, Tangen CM, Hussain MHA, et al. Docetaxel and estramustine compared with mitoxantrone and prednisone for advanced refractory prostate cancer. N Engl J Med 2004;351:1513 – 20.

39. Mattioli R, Lippe P, Massacesi C, et al. Long-survival in responding patients with metastatic breast cancer treated with doxorubicin-docetaxel combination. A multicentre phase II trial. Anticancer Res 2004;24:3257 – 61.

40. Lee YJ, Doliny P, Gomez-Fernandez C, Powell J, Reis I, Hurley J. Docetaxel and cisplatin as primary chemotherapy for treatment of locally advanced breast cancers. Clin Breast Cancer 2004;5:371 – 6.

41. Glasmacher A, Lilienfeld-Toal M. The current status of thalidomide in the management of multiple myeloma. Acta Haematol 2005;114:3 – 7.

42. Allegrini G, Paolo AD, Cerri E, et al. Irinotecan in combination with thalidomide in patients with advanced solid tumors: a clinical study with pharmacodynamic and pharmacokinetic evaluation. Cancer Chemother Pharmacol 2006;58:585 – 93.

43. Dahut WL, Gully JL, Arlen PM, et al. Randomized phase II trial of docetaxel plus thalidomide in androgen-independent prostate cancer. J Clin Oncol 2004;22:2532 – 9.

44. Heere-Ress E, Boehm J, Thallinger C, et al. Thalidomide enhances the anti-tumor activity of standard chemotherapy in a human melanoma xenotransplantation model. J Invest Dermatol 2005;125:201 – 6.

45. Shalli K, Brown I, Heys SD, Schofield AC. Alterations of β-tubulin isotypes in breast cancer cells resistant to docetaxel. FASEB J 2005;19: 1299 – 301.

46. Sève P, Mackey J, Isaac S, et al. Class III β-tubulin expression in tumor cells predicts response and outcome in patients with non-small cell lung cancer receiving paclitaxel. Mol Cancer Ther 2005;4: 2001 – 7.

47. Mozzetti S, Ferlini C, Concolino P, et al. III β-tubulin overexpression is a prominent mechanism of paclitaxel resistance in ovarian cancer patients. Clin Cancer Res 2005;11:298 – 305.

48. Urano N, Fujiwara Y, Doki Y, et al. Clinical significance of class III β-tubulin expression and its predictive value for resistance to docetaxel-based chemotherapy in gastric cancer. Int J Oncol 2006;28: 375 – 81.

49. Kavallaris M, Burkhart CA, Horwitz SB. Antisense oligonucleotides to class III β-tubulin sensitize drug-resistant cells to Taxol. Br J Cancer 1999; 80:1020 – 5.

50. Photiou A, Shah P, Leong LK, Moss J, Retsas S. *In vitro* synergy of paclitaxel (Taxol) and vinorelbine (Navelbine) against human melanoma cell lines. Eur J Cancer 1997;33:463 – 70.

51. Parimoo D, Jeffers S, Muggia FM. Severe neurotoxicity from vinorelbine-paclitaxel combinations. J Natl Cancer Inst 1996;88:1079 – 80.